Supplementary data

Table S1: Chromosomal runs of consecutive ORFs with a mean PB ratio more significantly deviated from that of the global distribution (Student's *t*-test, *p*-value $<5.10^{-4}$).

Chrom	ORF-ORF run	run length (# ORFs)	PB Mean (log_2)	t-test (p-value)
II	YBR103W-YBR139W	36	-0,31848	1,6721 E-04
II	YBR244W-YBR301W	58	-0,33373	1,6095 E-06
III	YCR044C-YCR077C	29	-0,49786	4,9051 E-04
IV	YDR218C-YDR237W	20	-0,46715	3,7978 E-04
IV	YDR328C-YDR348C	21	-0,66482	4,2498 E-04
VII	YGR004W-YGR028W	25	-0,47624	6,7106 E-05
VII	YGR272C-YGR294W	23	-0,65413	1,5177 E-05
IX	YIR020C-YIR037W	20	0,646550	4,7521 E-04
IX	YIR006C-YIR037W	34	0,518667	4,6228 E-04
X	YJR028W-YJR050W	23	0,742888	1,9800 E-04
XII	YLL021W-YLL01W	22	0,533677	4,9592 E-04
XIII	YMR056C-YMR086C	32	0,709341	4,9042 E-05
XIII	YMR145C-YMR183C	35	0,595785	2,6798 E-06

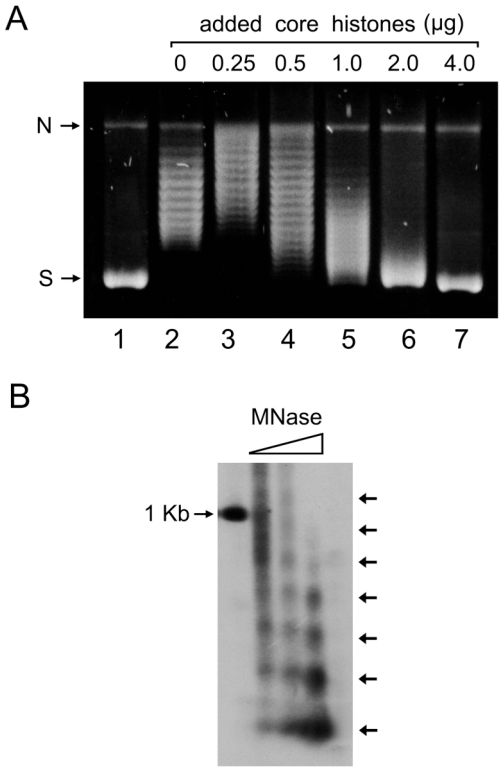

Figure S1. Chromatin assembly in plasmid YCp50. (A) Negatively supercoiled YCp50 plasmid (lane 1) was relaxed with vaccinia virus topoisomerase I (lane 2) and then incubated during 4 h at 35ºC, as described by Rodríguez-Campos et al. (ref. 39), with a whole-cell yeast extract supplemented with an ATP-regenerating system and increasing amounts of core histones purified from yeast chromatin (lanes 3-7, each containing 0.5 µg YCp50). After the reactions, the topology of deproteinized YCp50 was examined by electrophoresis in agarose gel containing TBE + 0.2µg/ml chloroquine. Migration of nicked (N) and supercoiled (S) forms of YCp50 is indicated. Reduction of DNA linking number (dLk) of the YCp50 topoisomer distribution allowed to estimate the nucleosomal density (nucleosomal DNA length/total DNA length) reached in each reaction, given that each assembled nucleosome constrains dLk~-1. For instance, in lane 4, about 20 nucleosomes were assembled since dLk~-20 (in this electrophoresis condition, the relaxed Lk distribution of lane 2 moves up and then folds down as Lk decreases). Nucleosomal DNA length/total DNA length was therefore ~0.35 (20x145/8000). B) Micrococcal nuclease digestion of assembled chromatin. To the YCp50 minichromosomes assembled above (lane 7), $CaCl_2$ and MNase were added and incubation was continued at room temperature. At different times, fractions of the digestion were removed and the examined by agarose-gel electrophoresis. A DNA length marker (1 Kb) and the positions of digested DNA fragments corresponding to 1, 2, 3, 4 5, 6, and 7 nucleosomes are indicated (arrows). Note that about 6 assembled nucleosomes per kb corresponds to a phasing ~165 bp, a typical value of native yeast chromatin.

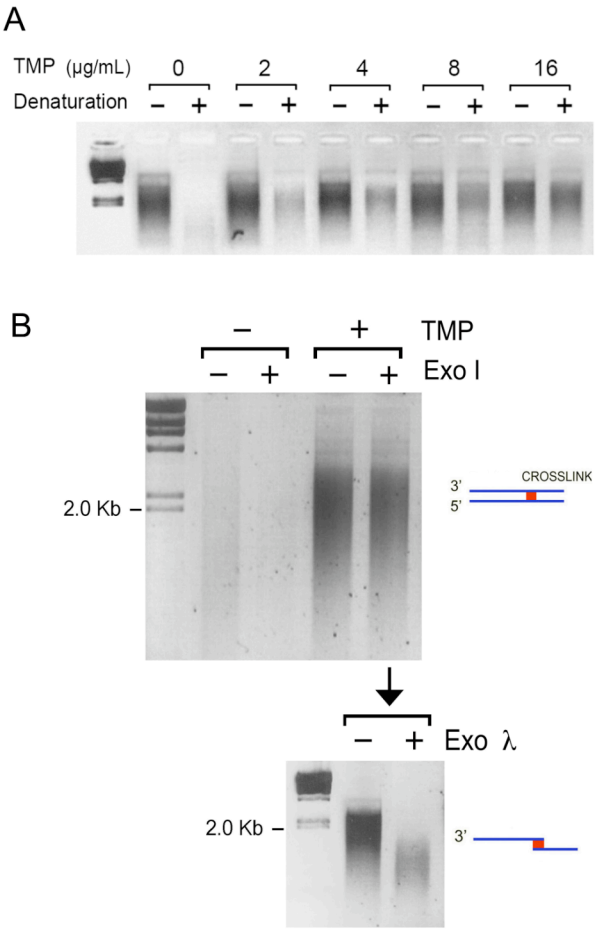

Figure S2. Calibration of *in vivo* DNA crosslinking and selection of crosslinked sequences**.** A) The yeast strain FY251 was incubated with increasing TMP concentrations, during 10 min, followed by irradiation with 360 nm light during 2 min, at a dose of 1.2 kJ/m^2/min. Total yeast DNA was extracted, fragmented and thermally denatured. Agarose gel electrophoresis showed how the fraction of DNA crosslinked fragments (those resistant to thermal denaturation) increased with TMP concentration. B) DNA fragments without and with TMP-mediated DNA crosslinks (-/+ TMP) were thermally denatured and digested with Exonuclease I. Crosslinked segments resistant to exonuclease I were then further digested by Exonuclease λ. As a result, crosslinked fragments were converted into a pair of single DNA chains covalently linked by a TMP molecule near their 5' ends.

Figure S3. PB ratios along *S. cerevisiae* chromosomes. The genomic dataset of PB ratios is plotted (log_2 scale being 0 the global mean) according to the ORF position ordering along the 16 chromosomes of *S. cerevisiae*. Student's *t*-test determined whether runs of consecutive ORFs had a mean PB ratio equal or statistically deviated from that of the global distribution. Chromosomal runs of consecutive ORFs with a high and low mean PB ratio (Student's *t*-test, *p*-value <10-3) are shadowed by yellow or pink boxes, respectively.

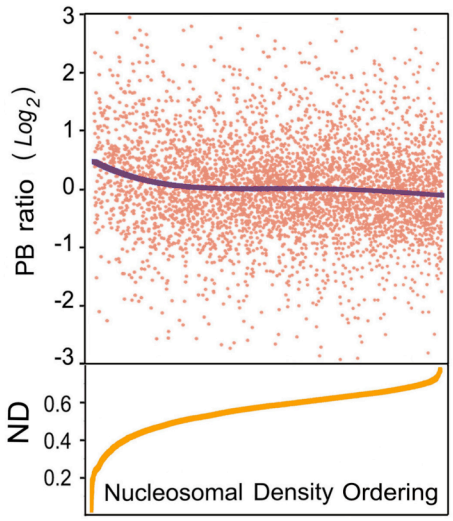

Figure S4. Lack of correlation of PB ratios with nucleosome density. The genomic distribution of PB ratios (log_2) is plotted according to the ranking of nucleosomal density (ND) of the gene corresponding to each array spot. The plot trendline (order 4 polynomial) is shown. Only a significant increase of PB values (Student's *t*-test, *p*-value $<10^{-5}$) was discernible for the subset of 500 genes with lowest ND.

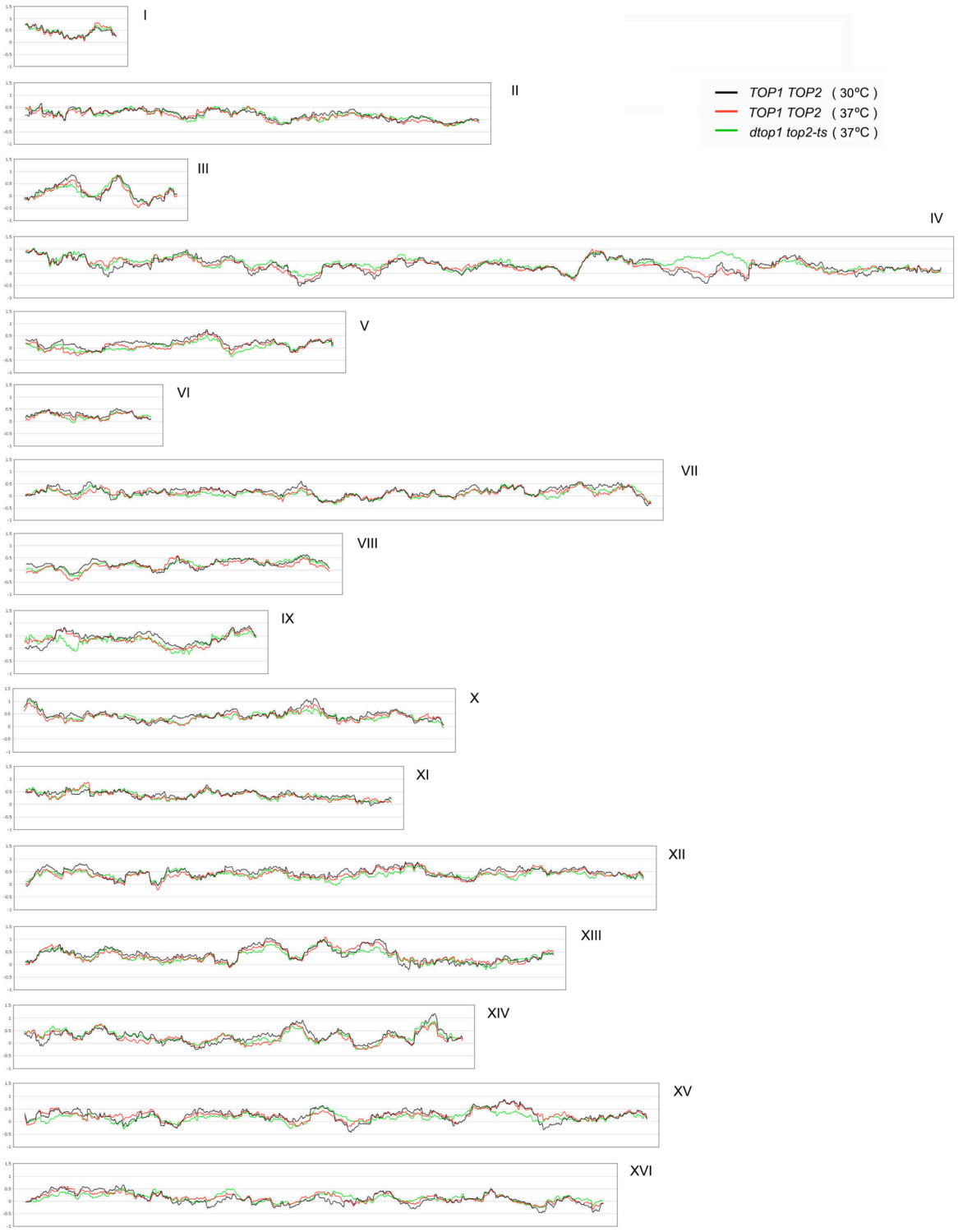

Figure S5: Chromosomal profiles of PB ratios and its alterations in topoisomerase deficient yeast cells. Regional profiles of PB ratios (log_2 scale being 0 the global mean) along each individual chromosome of *S. ce*revisiae are drawn by plotting sliding means of PB ratios in windows of 20 ORFs, moving one ORF at each step. Profiles obtained for *TOP1 TOP2* (at 30ºC and 37 ºC) and *Δtop1 top2^{ts}* (at 37ºC) yeast strains are compared.

Figure S6: Genome-wide alterations of PB ratios in topoisomerase deficient yeast cells. TMP photobinding changes are plotted along each individual chromosome of *S. cer*evisiae as the quotient of PB ratios obtained in *Δtop1 top2*^{ts} cells (at 37ºC) to those obtained in *TOP1 TOP2* cells (at 37ºC). Note the alterations spanning across large domains of Ch IV and Ch IX.

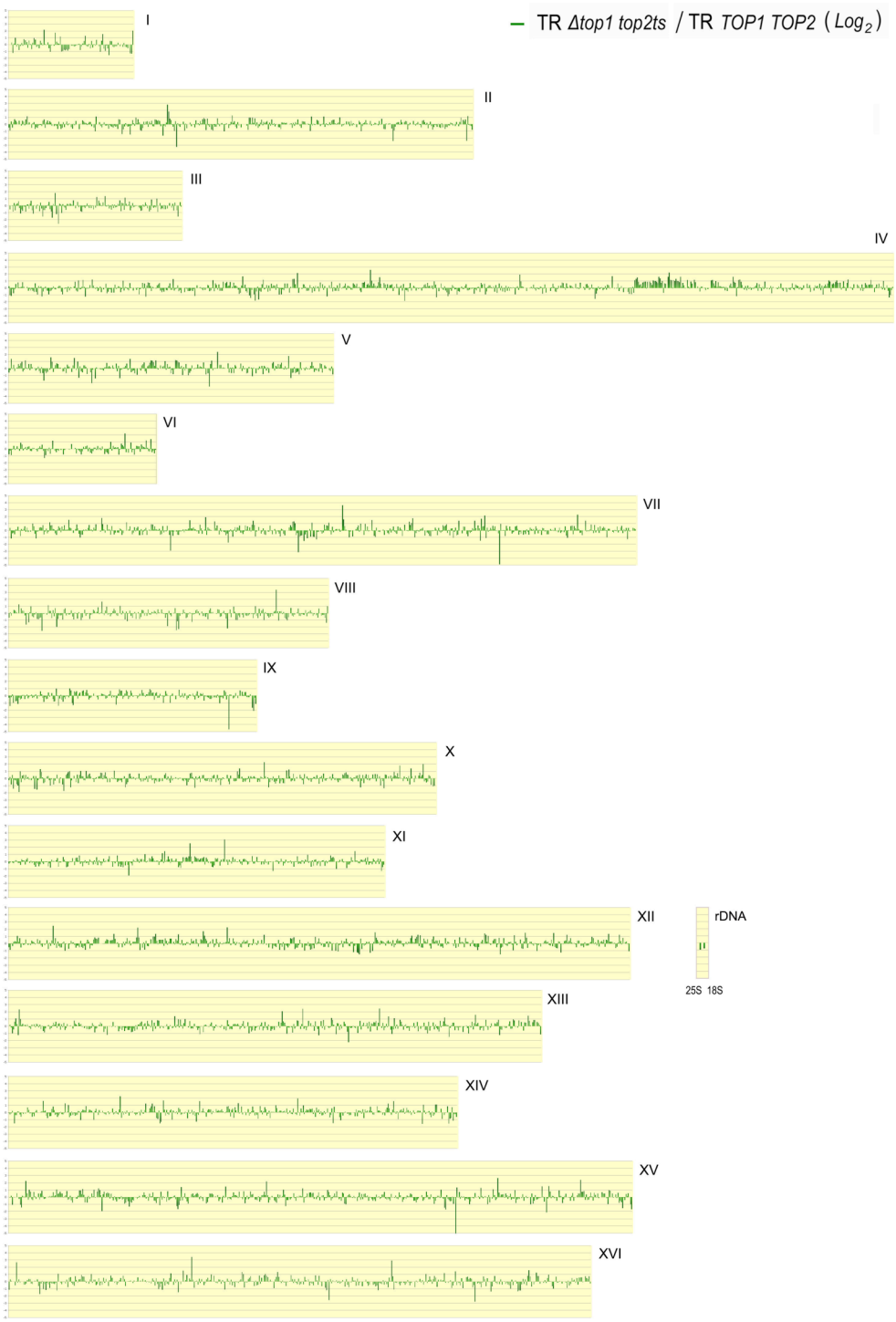

Figure S7: Genome-wide alterations of transcription rates in topoisomerase deficient yeast cells. Transcription changes are plotted along each individual chromosome of *S. ce*revisiae as ratios of TR values obtained in *Δtop1 top2*^{ts} cells (at 37ºC) to those obtained in *TOP1 TOP2* cells (at 37ºC). Note the burst of transcription along a large domain of Ch IV.